Personalized Medicine and Imaging

Clinical Cancer Research

Integrative Analysis Identifies a Novel AXL–PI3 Kinase–PD-L1 Signaling Axis Associated with Radiation Resistance in Head and Neck Cancer

Heath D. Skinner[1], Uma Giri[2], Liang P. Yang[3], Manish Kumar[3], Ying Liu[3], Michael D. Story[4], Curtis R. Pickering[5], Lauren A. Byers[2], Michelle D. Williams[6], Jing Wang[7], Li Shen[7], Suk Y. Yoo[7], You Hong Fan[7], David P. Molkentine[3], Beth M. Beadle[1], Raymond E. Meyn[3], Jeffrey N. Myers[5], and John V. Heymach[2]

Abstract

Purpose: The primary cause of death due to head and neck squamous cell carcinoma (HNSCC) is local treatment failure. The goal of this study was to examine this phenomenon using an unbiased approach.

Experimental Design: We utilized human papilloma virus (HPV)-negative cell lines rendered radiation-resistant (RR) via repeated exposure to radiation, a panel of HPV-negative HNSCC cell lines and three cohorts of HPV-negative HNSCC tumors ($n =$ 68, 97, and 114) from patients treated with radiotherapy and subjected to genomic, transcriptomic, and proteomic analysis.

Results: RR cell lines exhibited upregulation of several proteins compared with controls, including increased activation of Axl and PI3 kinase signaling as well as increased expression of PD-L1. Additionally, inhibition of either Axl or PI3 kinase led to decreased PD-L1 expression. When clinical samples were subjected to RPPA and mRNA expression analysis, PD-L1 was correlated with both Axl and PI3K signaling as well as dramatically associated with local failure following radiotherapy. This finding was confirmed examining a third cohort using immunohistochemistry. Indeed, tumors with high expression of PD-L1 had failure rates following radiotherapy of 60%, 70%, and 50% compared with 20%, 25%, and 20% in the PD-L1–low expression group ($P = 0.01$, 1.9×10^{-3}, and 9×10^{-4}, respectively). This finding remained significant on multivariate analysis in all groups. Additionally, patients with PD-L1 low/$CD8^+$ tumor-infiltrating lymphocytes high had no local failure or death due to disease ($P = 5 \times 10^{-4}$ and $P = 4 \times 10^{-4}$, respectively).

Conclusions: Taken together, our data point to a targetable Axl–PI3 kinase–PD-L1 axis that is highly associated with radiation resistance. *Clin Cancer Res; 23(11); 2713–22. ©2017 AACR.*

Introduction

Head and neck squamous cell carcinoma (HNSCC) leads to the death of more than 140,000 patients annually, primarily due to failure of local therapy, either surgery, radiotherapy or a combination of the two (1). Although advances in treatment, including the addition of cytotoxic chemotherapy to radiotherapy, have improved outcomes, approximately 30% to 50% of patients fail locally due to therapeutic resistance and ultimately succumb to their disease (2–4).

At present, the only effective biomarker of outcome in this tumor is the presence of human papilloma virus (HPV), which is associated with both improved response to therapy and outcome (5). Conversely, HPV-negative HNSCCs have far worse outcomes and lack clinically utilized biomarkers of response. Moreover, the addition of targeted agents to sensitize tumors to radiation in this disease has met with mixed results, with the most recent trial examining the addition of cetuximab showing no improvement over the current standard of care (2). Further, targetable alterations in HNSCC potentially leading to therapeutic resistance, such as PI3 kinase and Axl activation, as well as our own work examining focal adhesion kinase expression have been identified (6–8). However, the vast majority of this work has not taken into account the interaction between tumor and host immune response.

Although radiation is thought to be locally immunosuppressive due to the high radiosensitivity of lymphocytes, results from several studies have led investigators to postulate that the immune response is required for maximal response to radiation. Treatment with radiation can lead to enhanced MHC class 1 antigen expression (9) as well as increased numbers of antigen-presenting cells and interferon gamma secreting tumor-infiltrating lymphocytes (TIL; ref. 10). Further, in an *in vivo* model of melanoma, the

[1]Department of Radiation Oncology, The University of Texas MD Anderson Cancer Center, Houston, Texas. [2]Department of Thoracic and Head and Neck Medical Oncology, The University of Texas MD Anderson Cancer Center, Houston, Texas. [3]Department of Experimental Radiation Oncology, The University of Texas MD Anderson Cancer Center, Houston, Texas. [4]Simmons Comprehensive Cancer Center, Department of Radiation Oncology, The University of Texas Southwestern Medical Center, Dallas, Texas. [5]Department of Head and Neck Surgery, The University of Texas MD Anderson Cancer Center, Houston, Texas. [6]Department of Pathology, The University of Texas MD Anderson Cancer Center, Houston, Texas. [7]Department of Biostatistics, The University of Texas MD Anderson Cancer Center, Houston, Texas.

Note: Supplementary data for this article are available at Clinical Cancer Research Online (http://clincancerres.aacrjournals.org/).

Corresponding Author: Heath D. Skinner, The University of Texas MD Anderson Cancer Center, 1515 Holcombe Boulevard, Unit 97, Houston, TX 77030. Phone: 713-563-3508; Fax: 713-563-2331; E-mail: hskinner@mdanderson.org

doi: 10.1158/1078-0432.CCR-16-2586

Translational Relevance

Locoregional failure is the primary cause of death in head and neck cancer (HNSCC). Treatment of locally advanced HNSCC is typically composed of radiation in combination with either surgical resection and/or cytotoxic chemotherapy. Although human papilloma virus (HPV)-positive HNSCC is sensitive to radiation, HPV-negative tumors are comparatively resistant to this treatment. Thus, understanding potential, clinically targetable drivers of radioresistance in HPV-negative tumors is necessary to improve survival.

In the current study, we identified PD-L1 as significantly associated with locoregional failure following radiation in multiple cohorts of HPV-negative tumors. Interestingly, PD-L1 expression appears to be at least partly driven by Axl–PI3 kinase signaling. These data provide further support to incorporate agents that target PD-1/PD-L1 in combination with radiation in this patient population as well as provide potential selection criteria for these trials. Moreover, our data suggest that, in addition to direct antitumor effects, targeting either Axl or PI3 kinase may provide a benefit in regard to tumor immune response.

response to radiation is abrogated in the absence of functional T-lymphocytes (11). In additional preclinical models, blockade of PD-1/PD-L1 signaling led to improved efficacy of radiation (12).

Moreover, signaling cascades related to radioresistance have also been linked to tumor immune response. For example, Hwu and colleagues have recently shown that tumor loss of PTEN in melanoma leads to increased inhibition of a T-cell–mediated tumor response, with PI3 kinase inhibition at least partially reversing this phenomenon (13). Moreover, the epithelial-to-mesenchymal transition (EMT) has been linked to upregulation of immune checkpoints such as PD-L1 (14, 15). As EMT has been linked to both Axl and PI3 kinase activation as well as radiation resistance, it is possible that these signaling cascades may be driving both intrinsic radioresistance as well as inhibition of the tumor immune response necessary for radioresponse (16–18).

Despite these interesting preclinical data, the clinical significance of the interaction between tumor immunity and radioresponse is unclear, as are the tumor signaling events that modulate this interaction. In the current study, we utilized an integrated approach to examine this phenomenon and identified a potential modulation of PD-L1 expression via Axl–PI3K leading to clinical radioresistance and alterations in $CD8^+$ TIL response.

Materials and Methods

Study design

The objectives of this study were 2-fold. First, we wished to identify novel markers of resistance to radiation treatment in HPV-negative HNSCC using a combination of HNSCC cells engineered to be resistant to radiation via repeated exposure, a large bank of HPV-negative HNSCC cell lines and multiple cohorts of pretreatment HPV-negative HNSCC tumor specimens from patients treated uniformly (with surgery and postoperative radiation). These samples were subjected to proteomic and transcriptomic analysis using RPPA and mRNA expression array, respectively. Using this method, we identified PD-L1 as highly associated with treatment failure following radiation. We validated this finding using a third similarly treated patient cohort using targeted immunohistochemical (IHC) analysis. Secondly, we wished to explore upstream signaling to PD-L1 in HPV-negative HNSCC. This was performed using a combination of clinical specimens and *in vitro* analysis using chemical inhibition of potential upstream regulators of PD-L1.

Reverse phase protein array (RPPA)

Samples from similar HPV-negative HNSCC patients treated with surgical resection followed by postoperative radiation were analyzed via RPPA as described previously (19, 20). Tumor characteristics for this group are found in Supplementary Table S1. HPV-negative cell lines (48) were subjected to RPPA using the methodology described previously (8). To generate an induced radioresistance model, we subjected FADU HPV-negative HNSCC cells to 2 Gy twice a week for 4 weeks (FADU RR) cultured in parallel with unirradiated parental cells (FADU Parental). Cells were cultured and collected for baseline protein expression in triplicate and run in duplicate on RPPA as described previously (8). All cells were subjected to STR genotyping.

mRNA expression

Pretreatment surgical specimens from 97 HPV-negative HNSCC patients treated with surgery and postoperative radiation were examined for mRNA expression (Supplementary Table S2). Total RNA was extracted for clinical tumors and analyzed via Illumina mRNA expression array as described previously (8). llumina HumanWG-6 V3 BeadChip human whole-genome expression arrays (Illumina, Inc.) were used for RNA labeling and microarray hybridization. Following amplification and purification, each sample was hybridized for each array using standard Illumina protocols with streptavidin-Cy3 being used for detection. A total of 97 unique microarrays from 97 tumor specimens were processed for statistical analysis.

mRNA expression data from the Cancer Genome Atlas HPV-negative HNSCC cohort ($n = 243$) was also analyzed (21).

Tissue microarray (TMA)

A tissue microarray comprised of 114 of HNSCC was generated as described previously utilizing formalin-fixed paraffin-embedded (FFPE) tissue (22). All samples on the TMA represent surgical specimens of HNSCC patients treated with surgical resection followed by postoperative radiation, almost uniformly to 60 Gy. Tumor specimens were tested for p16 expression; those that were positive ($n = 12$) were excluded from the analysis (Supplementary Table S3). Immunohistochemical evaluation was performed on the TMA for all of the following markers utilizing standard techniques and the fully automated Leica Bond-Max stainers. The following antibodies were used: anti–PD-L1 (CD274; clone SP142, dilution 1:10), Spring Bioscience; refs. 23, 24); anti–PD-1 (1:100), anti-CD8 (1:20), and CD4 (1:25; Cell Marque). Scoring of all immune markers was performed by an experienced head and neck pathologist (M.D. Williams) and grouped and verified by a separate observer (U. Giri). The average value was utilized between tumor replicates. For PD-L1 expression, positive staining was independently determined within the tumor cells (0–100%) via cellular morphology. For CD4 and CD8, the number of positive lymphoid cells was quantitated within the tumor (TIL) was counted. PD-1 staining was scored as either

present, mixed (average of present and absent on duplicates) or absent. See Supplementary Fig. S1 for images of individual antibody staining.

Ion Torrent tumor sequencing

Isolated DNA was quantified by qPCR for Rnase P. Sequencing libraries were made from 10 ng of DNA with a custom AmpliSeq library containing 739 amplicons designed against the entire coding regions of 17 genes (CASP8, CCND1, CDKN2A, EGFR, FAT1, FBXW7, HLA-A, KEAP1, NFE2L2, NOTCH1, NOTCH2, NSD1, PIK3CA, TGFBR2, TP53, and TP63) and the mutation hotspots (G12/13 and Q61) in HRAS according to manufacturer's protocols. Samples were sequenced on Ion 318 chips to a depth of approximately 800×. Variants were called by using Ion Reporter software and manual filtering. HLA-A variants were ignored due to concerns about appropriate mapping.

Flow cytometry and immunoblot analysis

Flow-cytometric analysis of PD-L1 expression was performed as described previously (25). Briefly, cells at 70% to 80% confluency were trypsinized to obtain a single-cell suspension. Approximately 500,000 cells were washed with 2% FBS and resuspended in 100 μL 2% FBS and incubated with mouse anti-human PD-L1 (CD274) antibody that was directly conjugated with PE (1:200 dilution, Clone MIH1, BD Pharmingen) for 30 minutes at 4°C. Cells were then washed in 2% FBS and analyzed using a Gallios flow cytometer (Beckman Coulter) and FlowJo software (v.10.1). Prior to collection, cells were treated with either Bay 80-6946 (PI3 kinase inhibitor) or SGI-7079 (Axl inhibitor; both from Selleck Chemical) for 24 hours where indicated. Immunoblot analysis was performed as described previously (8). Commercially available siRNAs specific for either Axl or p110 PI3 kinase (GE Dharmacon) were transfected via electroporation (Nucleofector II, Amaxa) by using program T-001 with transfection agent T (Lonza). Cells were collected 48 to 72 hours after transfection and assayed as described above. Comparisons between treatment groups were performed using the Student t test, with $P < 0.05$ denoting significance.

Statistical analyses

For all patient groups, the optimal cutoff for PD-L1 group analysis was performed by generating a density plot of the staining distribution, which revealed a trimodal distribution. The high PD-L1 expression group was defined as the upper tertile, whereas the low PD-L1 expression group represents the remaining patients. Survival curves were generated by using the method of Kaplan–Meier, with log-rank statistics used to determine significance. Univariate analysis was performed using Cox regression. Variables with a $P < 0.1$ were included in the multivariate model and forward stepwise Cox regression was performed. R software, SPSS statistical software (v.20), JMP Pro (v.11.2.1) and GraphPad Prism were used.

Results

PD-L1 is upregulated in HNSCC cells with acquired radioresistance and modulated by Axl and PI3 kinase *in vitro*

As a first step toward identifying pathways associated with radioresistance, we exposed an HPV-negative HNSCC cell line to repeated 2-Gy doses of RT over a 4-week period, yielding a line that was significantly more radioresistant (FADU RR) than the parental cell from which it was derived (Supplementary Fig. S2). We then examined protein expression in these cells compared with the parental cell line (FADU parental) using RPPA. We observed Axl and p-Axl as well as markers of PI3K/AKT/mTOR pathway activation (phospho-AKT, phospho-GSK, and phosphoP70S6Kinase), and PD-L1 among the top proteins upregulated in FADU RR cells compared with parental line at an FDR of 0.1 (Fig. 1A and B). We confirmed the overexpression of several of these proteins via immunoblot and flow cytometry (Supplementary Fig. S3A and S3B).

To further explore potential interactions between these proteins *in vitro*, we examined RPPA data from 48 HPV-negative HNSCC cell lines (Fig. 1C). We observed significant correlation clustering between known downstream targets of PI3 kinase (Fig. 1C). We also observed that Axl was highly correlated with PD-L1 expression (Fig. 1C and D; Spearman r 0.68, $P = 1.16 \times 10^{-7}$). Although previously EMT and activation of PI3 kinase have been linked to radioresistance, the involvement of Axl and PD-L1 as well as their connection to one another and to radioresistance is unclear. To explore this, we examined PD-L1 expression via flow cytometry in OSC-19 HNSCC cells, which have high baseline expression of PD-L1 based on RPPA data (Fig. 1E; Supplementary Fig. S4A and S4B). Indeed, 73% of these cells had detectable expression of PD-L1 *in vitro*. We then treated these cells with either a chemical inhibitor of Axl or PI3 kinase. Either inhibitor led to substantially decreased PD-L1 expression compared with vehicle control, providing evidence for direct regulation of PD-L1 levels by both Axl and the PI3K pathway (Fig. 1E). A similar phenomenon was observed in another HPV-negative HNSCC cell line (SN2, Fig. 1F). Moreover, inhibition of either Axl or PI3 kinase using siRNA led to decreased PD-L1 expression in SN2 cells (Fig. 1G and H).

PD-L1 expression is associated with Axl and PI3 kinase signaling

To determine whether these *in vitro* observations could be validated clinically, and to further investigate the mechanism by which PD-L1 is upregulated in HPV-negative HNSCC, we examined tumors from a total of 68 patients with locally advanced HPV-negative HNSCC treated with surgery and postoperative radiotherapy via RPPA and evaluated for possible association with PD-L1 expression. Proteins and phospho-proteins significantly correlated with PD-L1 with an FDR of 0.1 are shown in Fig. 2A and C. These findings confirmed the clinical association between PD-L1, Axl, and the PI3K pathway.

To expand upon this finding, we assayed mRNA expression in a cohort of 97 HNSCC patients similarly treated with surgery and postoperative radiation. We then examined mRNA expression of proteins associated with PD-L1 expression on RPPA and correlated their mRNA expression with PD-L1 mRNA expression (Fig. 2B and C). Several molecules were correlated with PD-L1 expression at the proteomic and mRNA level, including Axl, the p85 subunit of PI3 kinase, pyruvate kinase muscle isozyme (PKM) and TRAIL. Moreover, in the TCGA HPV-negative Head and Neck cohort, Axl mRNA expression was significantly correlated with PD-L1 mRNA expression (Spearman $r = 0.3$, $P = 2 \times 10^{-6}$; Fig. 2D).

We then investigated whether activation of the PI3K pathway by *PIK3CA* mutation was also associated with an upregulation of PD-L1 (specific mutations for each cohort in Supplementary Table S4). Targeted sequencing for *PIK3CA* was performed in

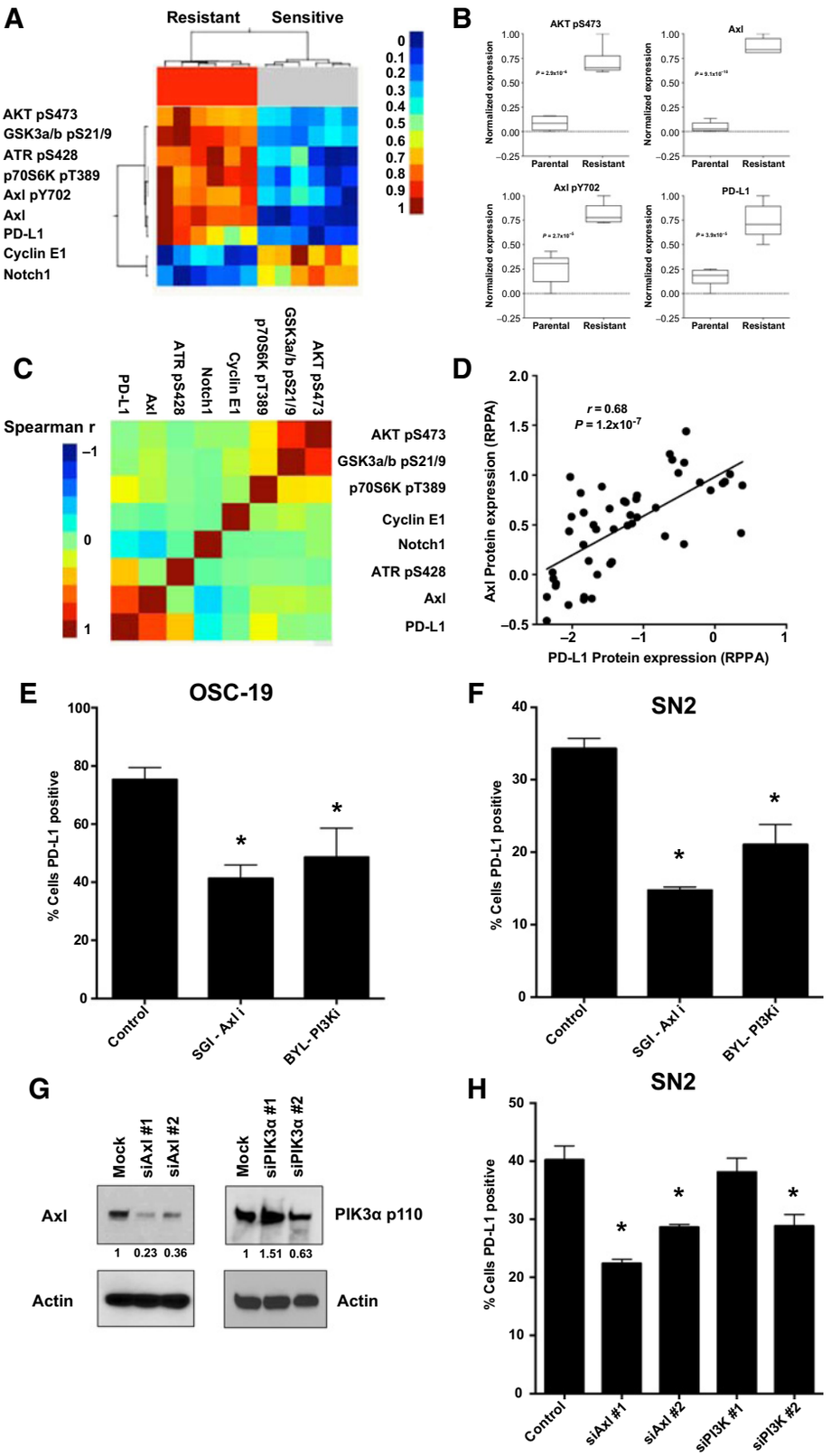

Figure 1.

PD-L1 expression is upregulated by Axl–PI3K signaling in an induced model of radioresistance. **A,** Unsupervised hierarchical cluster analysis of proteins and phospho-proteins from RPPA significantly different (FDR 0.05) between parental (FADU P) and induced radioresistant (FADU RR) cell lines (performed in triplicate). **B,** Protein expression from RPPA between FADU P and FACU RR for selected proteins. *P* values are for comparisons between FADU P and FADU RR for each protein. **C** and **D,** Correlation matrix for selected protein expression data from RPPA in 48 HPV-negative cell lines (**C**), with the correlation between PD-L1 and Axl expression from these data shown in **D**. **E** and **F,** Flow-cytometric analysis of PD-L1 positivity in OSC-19 HNSCC cells treated with vehicle, SGI-7079 (Axl inhibitor, 750 nmol/L) or Bay 80-6946 (PI3 kinase inhibitor 5 μmol/L) for 24 hours. **G,** Immunoblot following transfection of siRNA specific for either Axl or PI3 kinase p110, showing knockdown of Axl in both siRNAs utilized and p110 in one of the two siRNAs used. **H,** Flow-cytometic analysis of PD-L1 positivity shows inhibition of PD-L1 expression with effective siRNA-mediated knockdown of either Axl or PI3 kinase. This was not observed using siRNA construct against p110 that did not lead to p110 inhibition. *, $P < 0.05$ compared with control.

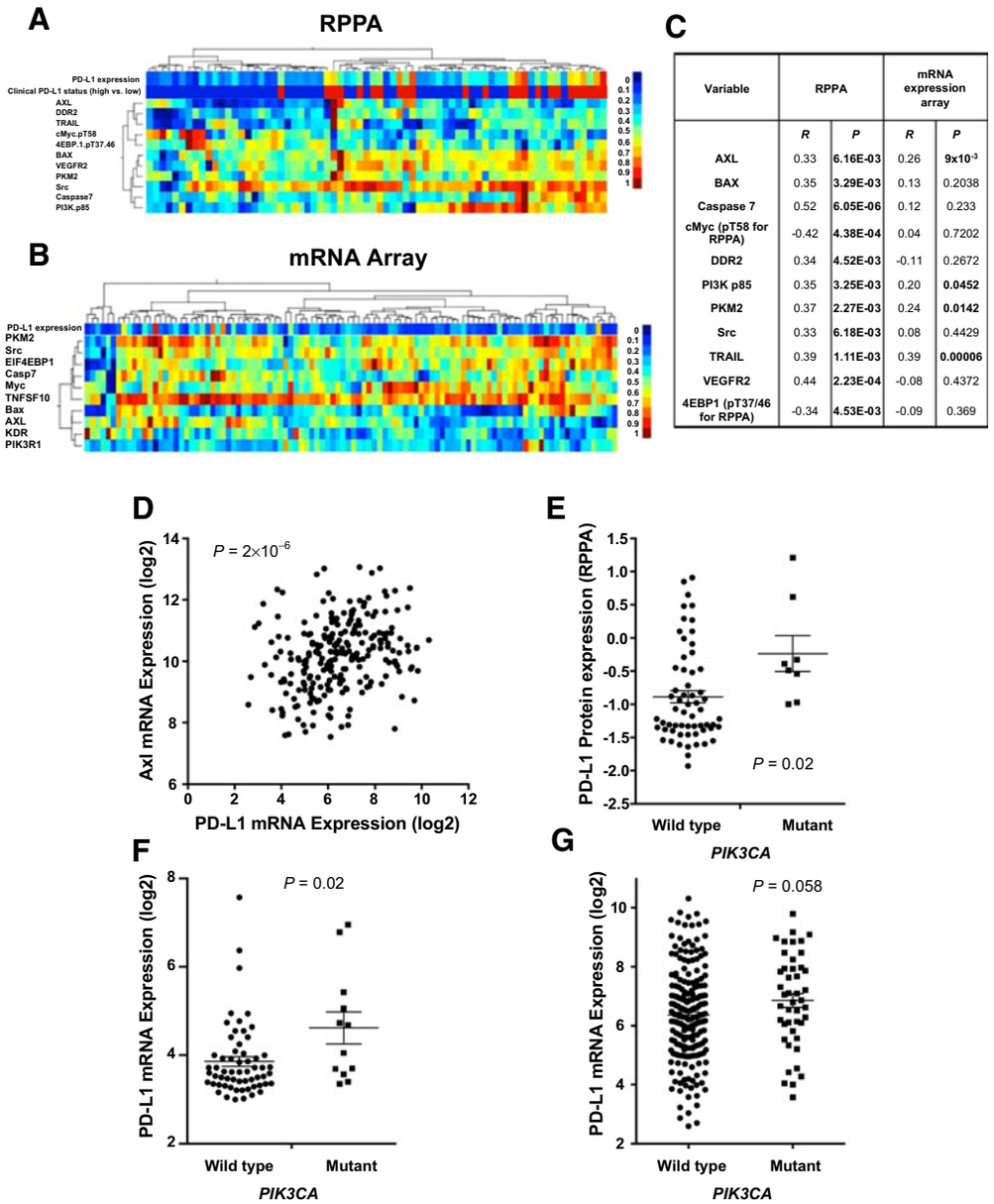

Variable	RPPA		mRNA expression array	
	R	*P*	*R*	*P*
AXL	0.33	**6.16E-03**	0.26	**$9x10^{-3}$**
BAX	0.35	**3.29E-03**	0.13	0.2038
Caspase 7	0.52	**6.05E-06**	0.12	0.233
cMyc (pT58 for RPPA)	-0.42	**4.38E-04**	0.04	0.7202
DDR2	0.34	**4.52E-03**	-0.11	0.2672
PI3K p85	0.35	**3.25E-03**	0.20	**0.0452**
PKM2	0.37	**2.27E-03**	0.24	**0.0142**
Src	0.33	**6.18E-03**	0.08	0.4429
TRAIL	0.39	**1.11E-03**	0.39	**0.00006**
VEGFR2	0.44	**2.23E-04**	-0.08	0.4372
4EBP1 (pT37/46 for RPPA)	-0.34	**4.53E-03**	-0.09	0.369

Figure 2.

PD-L1 expression is associated with Axl and PI3 kinase signaling. **A,** Hierarchical cluster analysis examining protein expression from clinical RPPA data correlated with PD-L1 (FDR = 0.1). **B,** Hierarchical cluster analysis of mRNA expression of targets identified in **A**. **C,** Spearman *r* and significance values from RPPA and mRNA array for correlation with PD-L1. **D,** Correlation between Axl and PD-L1 mRNA expression in the HPV-negative head and neck TCGA cohort (Spearman $r = 0.3$, $P = 2 \times 10^{-6}$). **E–G,** PD-L1 expression levels in *PIK3CA* wild-type and mutant tumors from the RPPA cohort (**E**; $P = 0.02$), mRNA cohort (**F**; $P = 0.02$), and the TCGA mRNA cohort (**G**; $P = 0.058$).

tumors for which tissue was available. Interestingly, both PD-L1 protein expression (Fig. 2E, $P = 0.02$) and mRNA expression (Fig. 2F, $P = 0.02$) were significantly greater in *PIK3CA* mutants versus wild-type. We examined PD-L1 mRNA expression in the TCGA HPV-negative cohort and PD-L1 mRNA trended toward higher expression levels in *PIK3CA* mutants (Fig. 2G; $P = 0.058$). Thus, in three HPV-negative HNSCC cohorts, Axl–PI3 kinase signaling was associated with PD-L1 expression.

RPPA identifies PD-L1 as a candidate biomarker of treatment failure following radiation

To determine the clinical significance of a potential Axl–PI3 kinase–PD-L1 axis, a univariate analysis of locoregional recurrence (LRR) of disease following radiation was performed for each protein on RPPA utilizing the Cox proportional hazards model. The results of this analysis are shown in Supplementary Table S5.

Table 1. Univariate analysis of LRR

Variable	Comparison	RPPA *P*	mRNA array *P*	IHC *P*
Tumor stage	T1-3 vs. T4	0.261	0.229	0.654
Nodal stage	N0-2a vs. >N2a	0.0987	0.129	0.001
Site		0.611	0.208	0.869
PD-L1	Continuous	0.003	4.4×10^{-4}	0.003
PD-1				0.758
CD8				0.224
CD4				0.626

Multivariate analysis of LRR

		RPPA		mRNA array		IHC	
Variable	**Comparison**	**HR (95% CI)**	***P***	**HR (95% CI)**	***P***	**HR (95% CI)**	***P***
Nodal stage	N0-2a vs. >N2a	3.54 (1.3–9.5)	0.012	2.05 (0.99–4.2)	0.05	3.05 (1.3–7.2)	0.011
PD-L1	Continuous	2.83 (1.6–5.0)	3.2×10^{-4}	1.95 (1.4–2.8)	1.6×10^{-4}	1.02 (1.002–1.02)	0.021

One of the most significant proteins associated with LRR was PD-L1 ($P = 0.0034$). On further analysis, including clinical variables, PD-L1 expression remained significantly associated with LRR (Table 1, $P = 3.2 \times 10^{-4}$). Further, 3 year LRR rate in patients with tumors expressing high levels of PD-L1 was 60%, compared with 20% in the low PD-L1 group (Fig. 3A, $P = 0.01$). PD-L1 expression was also significantly associated with disease-specific survival (DSS, $P = 0.04$), but had no association with distant metastasis (DM, $P = 0.8$).

Gene expression confirms PD-L1 as a biomarker of LRR

To further investigate the association between PD-L1 and radiation treatment failure in HPV-negative HNSCC, we performed univariate analysis for LRR in our mRNA expression data. Using Beta-Uniform Mixture (BUM) models for multiple testing adjustment, 8 genes were associated with LRR using a false discovery rate (FDR) of 0.1. The most striking finding was the high degree of significance of both PD-L1 ($P = 6.09 \times 10^{-05}$) and PD-L2 ($P = 1.10 \times 10^{-05}$) in predicting LRR following radiation in this patient population (Supplementary Table S6). Indeed, these two ligands were the 3rd and 8th most significant genes in the entire array associated with LRR. On multivariate analysis, including clinical variables, PD-L1 remained significantly associated with LRR (Table 1, $P = 1.6 \times 10^{-4}$). Three-year LRR rates were 70% in patients with high levels of PD-L1 mRNA expression, compared with 25% in the low PD-L1 group (Fig. 3B, $P = 1.9 \times 10^{-3}$).

PD-L1 staining is predictive of LRR

To validate the connection between radiation treatment failure and PD-L1 expression, we generated a tissue microarray (TMA) of tumor samples collected from patients with locally advanced HPV-negative HNSCC treated uniformly with surgery and postoperative radiotherapy. In these specimens, PD-L1 was found to be expressed at high levels in the tumor. PD-1, CD4-positive and CD8-positive immune cells were also observed and quantitated. The distribution of scores is shown in Supplementary Fig. S5. On univariate analysis, only tumor PD-L1 expression (Table 1, $P = 0.003$) and nodal stage ($P = 0.001$) were associated with LRR in this population. On multivariate analysis, both nodal stage ($P = 0.011$) and tumor PD-L1 expression ($P = 0.021$) remain associated with LRR. Three-year LRR rates were 50% in the PD-L1–high group compared with 20% in the PD-L1–low group ($P = 9 \times 10^{-4}$, Fig. 3C).

PD-L1 is predictive of LRR in HPV-negative HNSCC independent of p53 status

Prior studies have identified p53 mutation as a marker of treatment failure in HPV-negative HNSCC (26, 27). Thus, any prospective biomarker of radiation treatment failure in this population should account for p53 status. To this end, targeted sequencing was performed to determine p53 status in available tumors from the previously analyzed TMA ($n = 52$). PD-L1 expression remained associated with LRR in either a p53 wild-type or mutant context ($P = 0.002$ and $P = 0.014$ respectively; Supplementary Fig. S6A). Moreover, while the number of tumors with high PD-L1 expression was slightly lower in p53 wild-type tumors compared with p53 mutant tumors (20% of patients vs. 35% of patients), PD-L1 expression overall was similar in both p53 wild-type and mutant tumors (Supplementary Fig. S6B, $P = 0.3$), suggesting that the effect of PD-L1 on LRR is p53 independent.

PD-L1 expression and CD8-positive TILs modulate outcome following radiation

To further investigate the functional consequences of PD-L1 expression in HNSCC tumors, we also examined the correlation with subpopulations of TILs and other immune cell markers (Supplementary Table S7). A highly significant correlation was observed between CD8-positive TILs and tumor PD-L1 expression (Spearman $r = 0.45$, $P = 1.1 \times 10^{-6}$, Fig. 4A). Moreover, we also analyzed our mRNA expression data and found that CD8a mRNA expression was highly correlated with PD-L1 mRNA expression (Spearman $r = 0.45$, $P = 2 \times 10^{-6}$; Fig. 4B). This finding was confirmed in the HNSCC HPV-negative TCGA cohort (Fig. 4C).

To examine the association between CD8 infiltrate, PD-L1, and response to radiation, we established groups stratified by CD8-positive ($\geq$10 cells) and/or tumor PD-L1-positive ($\geq$30% of tumor-positive) patients based on IHC (Fig. 4D). Interestingly, PD-L1 remained predictive of outcome irrespective of CD8-positive immune infiltrate; however, patients who were CD8-positive, but PD-L1–negative ($n = 12$) had the best outcome compared with other patients, with no local failures ($P = 5 \times 10^{-4}$) and no death due to disease observed (4×10^{-4}).

Discussion

Radioresistance remains a major cause of treatment failure and mortality in HNSCC, and there is a significant unmet need for new markers and therapeutic targets to combat it. Here, using an

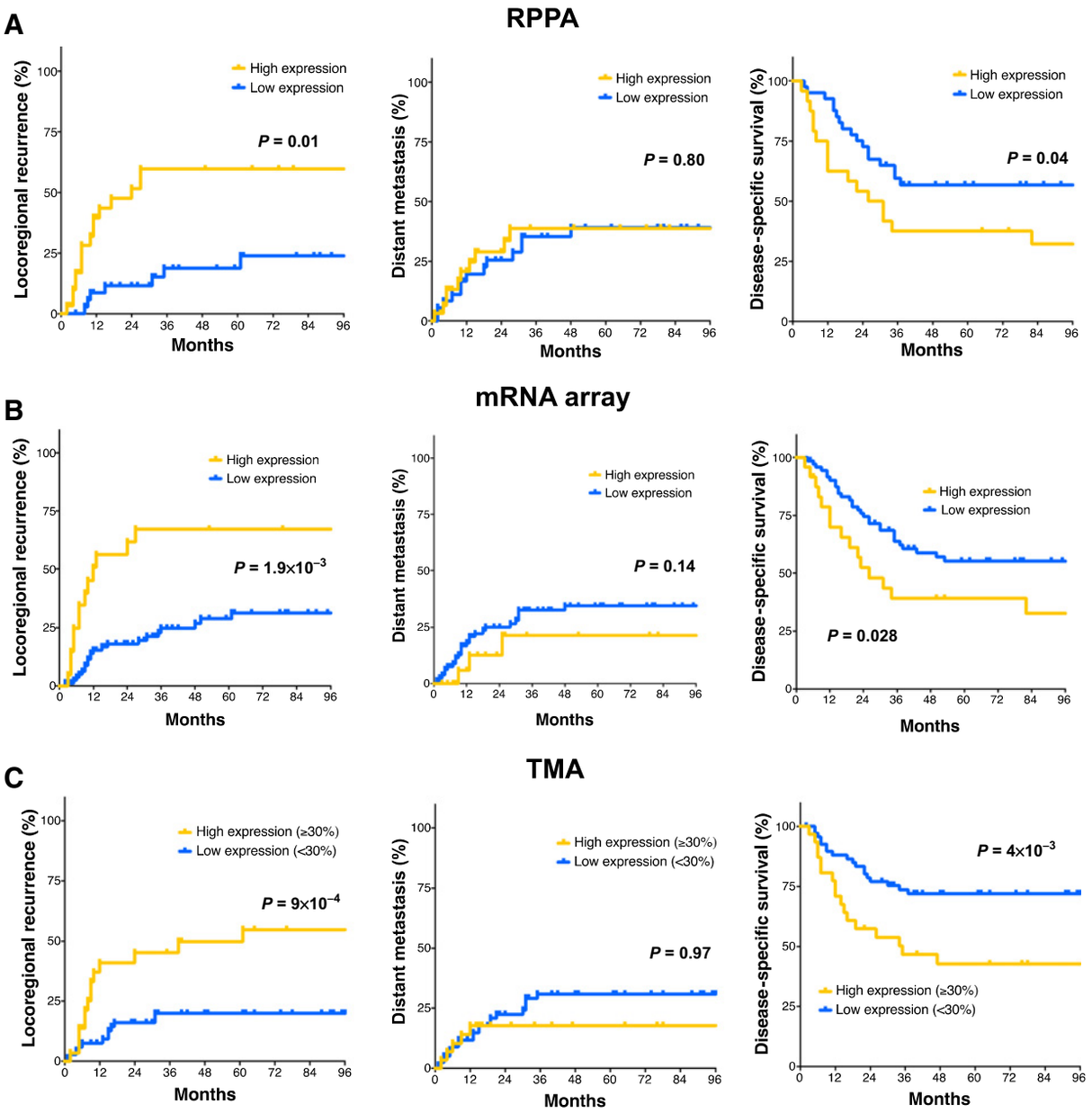

Figure 3.

PD-L1 expression is highly associated with LRR. **A–C,** Time to LRR, time to DM, or disease-specific survival in the RPPA (**A**) and mRNA expression (**B**) and TMA cohorts (**C**) by high versus low PD-L1 expression (see Materials and Methods for cutoff selection).

integrative analysis starting with preclinical models, we identify that Axl, the PI3K/Akt pathway, and PD-L1 are associated with radioresistance. Furthermore, Axl and the PI3K/AKT pathway are highly associated with, and appear to modulate, PD-L1 in HNSCC cells. Validating these associations clinically, we show that PD-L1 expression in resected tumors is associated with Axl and PI3K/Akt expression in HPV-negative HNSCC tumors, and is associated with LRR following radiotherapy in multiple patient cohorts, across multiple evaluation platforms.

Our initial studies were guided by the marked upregulation of PI3K, Axl, and PD-L1 expression in an acquired *in vitro* radiation resistance model. This is particularly interesting, in that this model was created in the absence of an immune response. Thus, it appears that the pathways upregulated during the acquisition of *in vitro* intrinsic radioresistance lead to a potential for immune evasion even without the contribution of the selective pressure of an immune-competent microenvironment. The association between Axl, PI3K, and PD-L1 observed in this model was

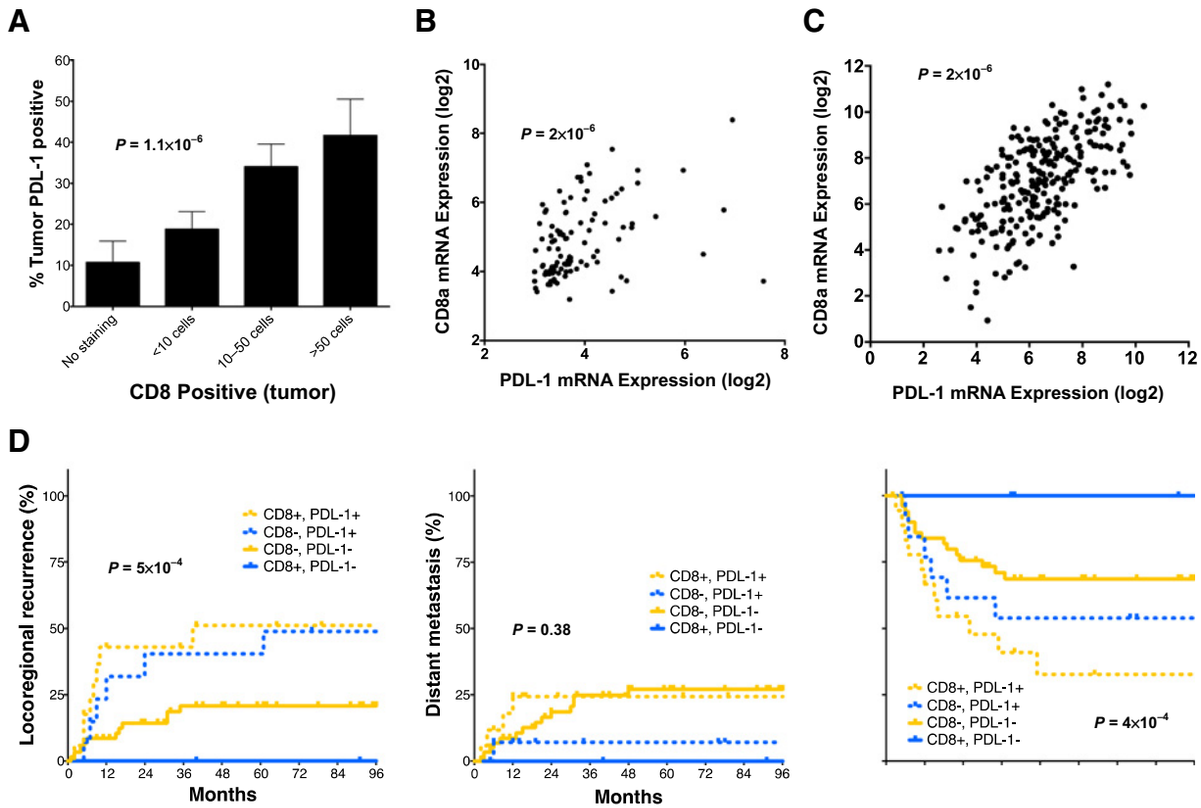

Figure 4.

The relationship between PD-L1 and CD8 immune infiltrate. **A,** Correlation between tumor PD-L1 staining and CD8-positive immune infiltrate (Spearman $r = 0.451$, $P = 1.1 \times 10^{-6}$) on TMA. **B** and **C,** The correlation between PD-L1 and CD8a mRNA expression from our institutional cohort (**B**; Spearman $r = 0.451$, $P = 2 \times 10^{-6}$) as well as correlation data for PD-L1 and CD8a in the HPV-negative head and neck TCGA cohort (**C**; CD8a, Spearman $r = 0.547$, $P = 2.1 \times 10^{-45}$; CD8b, Spearman $r = 0.444$, $P = 1 \times 10^{-28}$). **D,** Subset analysis of patients from the TMA cohort examining the relationship between CD8 and PD-L1 positivity on time to LRR, time to DM, or disease-specific survival.

consistent in a broad panel of cell lines as well as in multiple cohorts of clinical specimens examined via genomic, transcriptomic, and proteomic analysis. Moreover, inhibition of either PI3K or Axl led to significant reductions in PD-L1 expression under basal conditions.

The signaling events leading to PD-L1 expression, and ultimately tumor immune evasion, are far from clear. Although recent work has suggested that EGFR mRNA expression is associated with PD-L1 in HNSCC (28), in our RPPA cohort, neither EGFR protein expression or phosphorylation were associated with PD-L1 expression (Supplementary Table S5). Thus, the signaling pathways regulating PD-L1 expression remain to be explored.

One possible clue to the regulation of PD-L1 in these tumors may be found in the interaction between EMT and tumor immune response. Our group has observed upregulation of immune checkpoint markers, including PD-L1, in the context of the EMT phenotype in head and neck as well as non–small cell lung cancer (14, 29). Further, with regard to the connection between PD-L1 and EMT, it has been shown recently that upregulation of several genes associated with EMT, including Axl, is associated with resistance to PD-1 therapy in melanoma (30). Potential interactions between Axl and the PI3K pathway have previously been identified (31) and there is some evidence that the PI3K signaling network could control PD-L1 expression, albeit a definite link is still missing (32). These data, as well as the work presented herein, point to a functional link between PI3K activation and Axl, leading to higher levels of PD-L1 expression, both *in vitro* and clinically.

Once expressed on the cancer cell, the relationship between PD-L1 and the response to radiation is also not well explored in HPV-negative HNSCC. We found PD-L1 to be highly enriched in HPV-negative HNSCC cells engineered to be radioresistant via continued radiation challenge, while our clinical studies identified a dramatic association between PD-L1 and failure following radiotherapy via unbiased screening of both protein expression via RPPA, mRNA expression array as well as a validation via IHC. In all patient cohorts, high baseline expression of PD-L1 was associated with dramatically increased risk of LRR. Interestingly, this was in the absence of alterations in the rate of distant metastasis in three different cohorts of patients, which argues for a primary interaction in this disease site between radiotherapy outcome and immune response.

In regard to the interplay between the host immune response and tumor PD-L1 expression, it is known that $CD8^+$ T cells can induce PD-L1 upregulation in multiple tumor types both *in vitro*

and *in vivo* (33, 34). Consistent with that observation, we found that $CD8^+$ T-cell infiltration at the time of surgical resection was significantly correlated with tumor PD-L1 expression in multiple patient cohorts. Thus, in this tumor type, PD-L1 overexpression may be at least partially induced as opposed to a completely intrinsic phenomenon, at least in the context of an intact tumor. This study cannot comment on the expression of PD-L1 in the setting of microscopic disease remaining following resection, nor changes in PD-L1 expression during radiotherapy; however, based upon the strong association between resected tumor PD-L1 expression and outcome following radiotherapy it appears that PD-L1 expression and T-cell infiltrate at the time of surgical resection does indeed affect response following radiotherapy. It is possible that the population of $CD8^+$ T cells within PD-L1–positive tumors represents exhausted T cells instead of antitumorigenic cytotoxic infiltrate (35, 36). The mechanism for this relationship between potentially exhausted T cells and tumor PD-L1 is unclear at this point. It is possible that infiltration of tumor parenchyma by cytotoxic $CD8^+$ T cells and consequent production of IFNγ would induce PD-L1 upregulation (33, 37, 38), via upregulation of PI3K and Axl, which in turn could lead to T-cell exhaustion (39, 40).

In conclusion, in the current study we identified and validated PD-L1 as a significant biomarker of treatment failure in HPV-negative HNSCC following radiotherapy using both screening approaches as well as targeted IHC. This phenomenon appears to be linked to Axl/PI3 kinase signaling within the tumor. These findings provide a strong rationale for the combination of immune checkpoint blockade and radiation in this setting, as well as potentially utilizing Axl or PI3 kinase blockade to affect both tumor radiosensitization and immune response.

Disclosure of Potential Conflicts of Interest

M.D. Story reports receiving commercial research grants from Galera Therapeutics, Inc. and Novocure and is a consultant/advisory board member for Galera Therapeutics, Inc. J.V. Heymach is a consultant/advisory board member for ARIAD Pharmaceuticals, Inc., AstraZeneca, Boehringer Ingelheim, Bristol-Myers Squibb, EMD Serono, Genentech, Inc., Jounce Therapeutics, and Novartis International AG. No potential conflicts of interest were disclosed by the other authors.

Authors' Contributions

Conception and design: H.D. Skinner, J.V. Heymach
Development of methodology: H.D. Skinner, M. Kumar, J.V. Heymach
Acquisition of data (provided animals, acquired and managed patients, provided facilities, etc.): H.D. Skinner, U. Giri, L.P. Yang, M.D. Story, C.R. Pickering, L.A. Byers, M.D. Williams, Y.H. Fan, D.P. Molkentine, B.M. Beadle, J.V. Heymach
Analysis and interpretation of data (e.g., statistical analysis, biostatistics, computational analysis): H.D. Skinner, L.P. Yang, C.R. Pickering, L.A. Byers, J. Wang, L. Shen, S.Y. Yoo, B.M. Beadle, J.V. Heymach
Writing, review, and/or revision of the manuscript: H.D. Skinner, M. Kumar, M.D. Story, L.A. Byers, M.D. Williams, B.M. Beadle, R.E. Meyn, J.V. Heymach
Administrative, technical, or material support (i.e., reporting or organizing data, constructing databases): L.P. Yang
Study supervision: H.D. Skinner, M. Kumar, J.V. Heymach

Grant Support

This work was supported by grants from the NCI (NIH): R01 CA 168484-022 (J.V. Heymach), HNSCC SPORE 5 P50CA070907-16 (J.V. Heymach and J.N. Myers), CCSG 5 P30 CA01667239 (J.V. Heymach), R01 CA 168485 (R.E. Meyn), and R21 CA 182964 (H.D. Skinner). This work was also supported by the Cancer Prevention Institute of Texas (RP150293; H.D. Skinner) and the Center for Radiation Oncology Research (Seed Grant; H.D. Skinner and C.R. Pickering) through generous support from Mr. and Mrs. William Dr. Rollnick.

The costs of publication of this article were defrayed in part by the payment of page charges. This article must therefore be hereby marked *advertisement* in accordance with 18 U.S.C. Section 1734 solely to indicate this fact.

Received October 17, 2016; revised November 18, 2016; accepted February 16, 2017; published OnlineFirst May 5, 2017.

References

1. Torre LA, Bray F, Siegel RL, Ferlay J, Lortet-Tieulent J, Jemal A. Global cancer statistics, 2012. CA Cancer J Clin 2015;65:87–108.
2. Ang KK, Zhang Q, Rosenthal DI, Nguyen-Tan PF, Sherman EJ, Weber RS, et al. Randomized phase III trial of concurrent accelerated radiation plus cisplatin with or without cetuximab for stage III to IV head and neck carcinoma: RTOG 0522. J Clin Oncol 2014;32:2940–50.
3. Harari PM, Harris J, Kies MS, Myers JN, Jordan RC, Gillison ML, et al. Postoperative chemoradiotherapy and cetuximab for high-risk squamous cell carcinoma of the head and neck: Radiation Therapy Oncology Group RTOG-0234. JCO 2014;32:2486–95.
4. Nguyen-Tan PF, Zhang Q, Ang KK, Weber RS, Rosenthal DI, Soulieres D, et al. Randomized phase III trial to test accelerated versus standard fractionation in combination with concurrent cisplatin for head and neck carcinomas in the Radiation Therapy Oncology Group 0129 Trial: Long-Term Report of Efficacy and Toxicity. JCO 2014;32:3858–67.
5. Ang KK, Harris J, Wheeler R, Weber R, Rosenthal DI, Nguyen-Tan PF, et al. Human papillomavirus and survival of patients with oropharyngeal cancer. N Engl J Med 2010;363:24–35.
6. Brand TM, Iida M, Stein AP, Corrigan KL, Braverman CM, Coan JP, et al. AXL is a logical molecular target in head and neck squamous cell carcinoma. Clin Cancer Res 2015;21:2601–12.
7. Bussink J, van der Kogel AJ, Kaanders JHAM. Activation of the PI3-K/AKT pathway and implications for radioresistance mechanisms in head and neck cancer. Lancet Oncol 2008;9:288–96.
8. Skinner HD, Giri U, Yang L, Woo SH, Story MD, Pickering CR, et al. Proteomic profiling identifies PTK2/FAK as a driver of radioresistance in HPV negative head and neck cancer. Clin Cancer Res 2016;22:4643–50.
9. Reits EA, Hodge JW, Herberts CA, Groothuis TA, Chakraborty M, K. Wansley E, et al. Radiation modulates the peptide repertoire, enhances MHC class I expression, and induces successful antitumor immunotherapy. J Exp Med 2006;203:1259–71.
10. Lugade AA, Moran JP, Gerber SA, Rose RC, Frelinger JG, Lord EM. Local radiation therapy of B16 melanoma tumors increases the generation of tumor antigen-specific effector cells that traffic to the tumor. J Immunol 2005;174:7516–23.
11. Lee Y, Auh SL, Wang Y, Burnette B, Wang Y, Meng Y, et al. Therapeutic effects of ablative radiation on local tumor require $CD8^+$ T cells: changing strategies for cancer treatment. Blood 2009;114:589–95.
12. Deng L, Liang H, Burnette B, Beckett M, Darga T, Weichselbaum RR, et al. Irradiation and anti-PD-L1 treatment synergistically promote antitumor immunity in mice. J Clin Invest 2014;124:687–95.
13. Peng W, Chen JQ, Liu C, Malu S, Creasy C, Tetzlaff MT, et al. Loss of PTEN promotes resistance to T cell-mediated immunotherapy. Cancer Discov 2016;6:202–16.
14. Lou Y, Diao L, Parra Cuentas ER, Denning WL, Chen L, Fan YH, et al. Epithelial–mesenchymal transition is associated with a distinct tumor microenvironment including elevation of inflammatory signals and multiple immune checkpoints in lung adenocarcinoma. Clin Cancer Res 2016;22:3630–42.
15. Ock C-Y, Kim S, Keam B, Kim M, Kim TM, Kim J-H, et al. PD-L1 expression is associated with epithelial–mesenchymal transition in head and neck squamous cell carcinoma. Oncotarget 2016;7:15901–14.
16. Byers LA, Diao L, Wang J, Saintigny P, Girard L, Peyton M, et al. An epithelial–mesenchymal transition gene signature predicts resistance to

EGFR and PI3K inhibitors and identifies Axl as a therapeutic target for overcoming EGFR inhibitor resistance. Clin Cancer Res 2013; 19:279–90.
17. Yang Y, Ahn Y-H, Chen Y, Tan X, Guo L, Gibbons DL, et al. ZEB1 sensitizes lung adenocarcinoma to metastasis suppression by PI3K antagonism. J Clin Invest 2014;124:2696–708.
18. Marie-Egyptienne DT, Lohse I, Hill RP. Cancer stem cells, the epithelial to mesenchymal transition (EMT) and radioresistance: potential role of hypoxia. Cancer Lett 2013;341:63–72.
19. Skoulidis F, Byers LA, Diao L, Papadimitrakopoulou VA, Tong P, Izzo J, et al. Co-occurring genomic alterations define major subsets of KRAS-mutant lung adenocarcinoma with distinct biology, immune profiles, and therapeutic vulnerabilities. Cancer Discov 2015;5:860–77.
20. Byers LA, Wang J, Nilsson MB, Fujimoto J, Saintigny P, Yordy J, et al. Proteomic profiling identifies dysregulated pathways in small cell lung cancer and novel therapeutic targets including PARP1. Cancer Discov 2012;2:798–811.
21. The Cancer Genome Atlas Network. Comprehensive genomic characterization of head and neck squamous cell carcinomas. Nature 2015;517: 576–82.
22. Moeller BJ, Yordy JS, Williams MD, Giri U, Raju U, Molkentine DP, et al. DNA repair biomarker profiling of head and neck cancer: Ku80 expression predicts locoregional failure and death following radiotherapy. Clin Cancer Res 2011;17:2035–43.
23. Herbst RS, Soria J-C, Kowanetz M, Fine GD, Hamid O, Gordon MS, et al. Predictive correlates of response to the anti-PD-L1 antibody MPDL3280A in cancer patients. Nature 2014;515:563–7.
24. Powles T, Eder JP, Fine GD, Braiteh FS, Loriot Y, Cruz C, et al. MPDL3280A (anti-PD-L1) treatment leads to clinical activity in metastatic bladder cancer. Nature 2014;515:558–62.
25. Rosenblatt J, Glotzbecker B, Mills H, Vasir B, Tzachanis D, Levine JD, et al. PD-1 blockade by CT-011, anti-PD-1 antibody, enhances ex vivo T-cell responses to autologous dendritic cell/myeloma fusion vaccine. J Immunother 2011;34:409–18.
26. Poeta ML, Manola J, Goldwasser MA, Forastiere A, Benoit N, Califano JA, et al. TP53 mutations and survival in squamous-cell carcinoma of the head and neck. N Engl J Med 2007;357:2552–61.
27. Skinner HD, Sandulache VC, Ow TJ, Meyn RE, Yordy JS, Beadle BM, et al. TP53 disruptive mutations lead to head and neck cancer treatment failure through inhibition of radiation-induced senescence. Clin Cancer Res 2012;18:290–300.
28. Concha-Benavente F, Srivastava RM, Trivedi S, Lei Y, Chandran U, Seethala RR, et al. Identification of the cell-intrinsic and -extrinsic pathways downstream of EGFR and IFNγ that induce PD-L1 expression in head and neck cancer. Cancer Res 2016;76:1031–43.
29. Mak MP, Tong P, Diao L, Cardnell RJ, Gibbons DL, William WN, et al. A patient-derived, pan-cancer EMT signature identifies global molecular alterations and immune target enrichment following epithelial-to-mesenchymal transition. Clin Cancer Res 2016;22:609–20.
30. Hugo W, Zaretsky JM, Sun L, Song C, Moreno BH, Hu-Lieskovan S, et al. Genomic and transcriptomic features of response to anti-PD-1 therapy in metastatic melanoma. Cell 2016;165:35–44.
31. Dufies M, Jacquel A, Belhacene N, Robert G, Cluzeau T, Luciano F, et al. Mechanisms of AXL overexpression and function in Imatinib-resistant chronic myeloid leukemia cells. Oncotarget 2011;2:874–85.
32. Atefi M, Avramis E, Lassen A, Wong DJL, Robert L, Foulad D, et al. Effects of MAPK and PI3K pathways on PD-L1 expression in melanoma. Clin Cancer Res 2014;20:3446–57.
33. Shi F, Shi M, Zeng Z, Qi R-Z, Liu Z-W, Zhang J-Y, et al. PD-1 and PD-L1 upregulation promotes CD8(+) T-cell apoptosis and postoperative recurrence in hepatocellular carcinoma patients. Int J Cancer 2011;128:887–96.
34. Tumeh PC, Harview CL, Yearley JH, Shintaku IP, Taylor EJM, Robert L, et al. PD-1 blockade induces responses by inhibiting adaptive immune resistance. Nature 2014;515:568–71.
35. Sfanos KS, Bruno TC, Meeker AK, De Marzo AM, Isaacs WB, Drake CG. Human prostate-infiltrating CD8$^+$ T lymphocytes are oligoclonal and PD-1+. Prostate 2009;69:1694–703.
36. Ahmadzadeh M, Johnson LA, Heemskerk B, Wunderlich JR, Dudley ME, White DE, et al. Tumor antigen-specific CD8 T cells infiltrating the tumor express high levels of PD-1 and are functionally impaired. Blood 2009;114:1537–44.
37. Lee S-J, Jang B-C, Lee S-W, Yang Y-I, Suh S-I, Park Y-M, et al. Interferon regulatory factor-1 is prerequisite to the constitutive expression and IFN-gamma-induced upregulation of B7-H1 (CD274). FEBS Lett 2006; 580:755–62.
38. Abiko K, Matsumura N, Hamanishi J, Horikawa N, Murakami R, Yamaguchi K, et al. IFN-γ from lymphocytes induces PD-L1 expression and promotes progression of ovarian cancer. Br J Cancer 2015;112:1501–9.
39. Day CL, Kaufmann DE, Kiepiela P, Brown JA, Moodley ES, Reddy S, et al. PD-1 expression on HIV-specific T cells is associated with T-cell exhaustion and disease progression. Nature 2006;443:350–4.
40. Wherry EJ. T cell exhaustion. Nat Immunol 2011;12:492–9.